atmosphere

MDPI

Article

Changes in Regional Circulation Weather Type in Morocco During the Period 1980–2019

Jaafar El Kassioui [1], Mohamed Hanchane [1], Nir Y. Krakauer [2,3,*], Laïla Amraoui [4] and Ridouane Kessabi [1]

[1] Laboratoire Territoire Patrimoine et Histoire, Department of Geography, Faculty of Letters and Human Sciences Dhar El-Mehraz, Sidi Mohamed Ben Abdellah University, Fez 30050, Morocco; jaafar.elkassioui@usmba.ac.ma (J.E.K.); mohamed.hanchane@usmba.ac.ma (M.H.); ridouane.kessabi@usmba.ac.ma (R.K.)
[2] Department of Civil Engineering, The City College of New York, City University of New York, New York, NY 10031, USA
[3] Department of Earth and Environmental Sciences, City University of New York Graduate Center, New York, NY 10031, USA
[4] Laboratory of Studies and Research in Geography, Department of Geography, Faculty of Letters and Human Sciences, Moulay Ismail University, Meknes 50000, Morocco; l.amraoui@umi.ac.ma
* Correspondence: nkrakauer@ccny.cuny.edu

Abstract

Morocco is among the regions in the Mediterranean basin most exposed to the impacts of climate variability and change. This increasing exposure requires a detailed and rigorous analysis of regional atmospheric dynamics to better understand the mechanisms behind recent climate trends. This study aims to examine the variability of circulation weather types (CWTs) at a regional scale over the period 1980–2019, within a geographical area bounded by latitudes 20° to 40° N and longitudes 10° to 22.5° W. The analysis is based on data from the NCEP-DOE Reanalysis 2, including mean sea level pressure (MSLP) and geopotential height at 500 hPa (Z500), with a spatial resolution of 2.5° in both latitude and longitude. The adopted methodology identifies daily CWT using a principal component analysis (PCA) in S-mode with Varimax rotation (PCAV), followed by the evaluation of their monthly distributions and temporal trends. The analysis highlights a marked trend toward increased atmospheric configurations conducive to hot conditions during the dry season, associated with the intensification and northward shift in the Saharan thermal low. This dynamic is reinforced by the increased frequency of ridges or high geopotential heights at 500 hPa, which transport warm tropical air toward the region. Moreover, the study reveals a notable decrease in the frequency of upper-level troughs at 500 hPa during the wet season. These upper-level troughs play a crucial role in cyclogenesis and the delivery of precipitation. These findings indicate a shift toward a regional atmospheric dynamic unfavorable to Morocco's hydric balance, characterized by more frequent and intense summer heat and worsening winter drought.

Keywords: circulation weather types (CWT); mean sea level pressure (MSLP); 500 hPa pessure level (Z500); NCEP-DOE Reanalysis 2; annual CWT trends

Academic Editor: Nicola Scafetta

Received: 31 March 2026
Revised: 20 April 2026
Accepted: 23 April 2026
Published: 28 April 2026

1. Introduction

Anthropogenic climate change is driving a significant increase in the frequency and intensity of extreme weather and climate events. These changes are primarily fueled by greenhouse gas emissions, which have led to a substantial rise in global temperatures. Specifically, the global surface temperature increased by 1.1 °C during the 2011–2020 period

compared to the 1850–1900 baseline [1]. In the future, this global warming is projected to manifest even more severely in the Mediterranean basin. Under the RCP8.5 scenario, regional temperatures are expected to rise by up to 5.6 °C by the end of the 21st century—a warming rate that exceeds the global average by approximately 20% [2].

Recent research within the Mediterranean Basin underscores that anthropogenically induced climate change will trigger substantial perturbations in both socio-economic and ecological systems. Specifically, this trajectory is evidenced by a marked contraction in freshwater availability and exacerbated hydrological stress [3], coupled with an increased prevalence of forest fires [4]. Regarding Morocco, future projections indicate a drastic decline in water resources by 2080, with estimated reductions ranging from 23% to 51% [5]. Consequently, elucidating the atmospheric driving mechanisms behind these shifts in Morocco is of paramount importance. In this context, therefore, circulation weather types (CWTs) play a fundamental role in understanding regional climate variability [6,7]. A systematic analysis of the frequency and long-term trends of CWTs offers a robust diagnostic perspective on the climatic evolution of the Mediterranean, enabling rigorous scientific comparisons with other sub-regions across the basin.

The methods for classifying these types have evolved, and their applications in meteorology and climatology have expanded [8]. Numerous studies have investigated atmospheric circulation at synoptic and seasonal scales through the analysis of weather regimes [9–12]. It is necessary to refine the spatial scale to describe circulation patterns more accurately as they contribute to climatic variables—such as temperature and precipitation—at specific locations of interest [13]. In connection with this scale reduction from global to regional, several methods and approaches have been developed to produce coherent and relevant classifications.

The classification of circulation weather types has a long-standing tradition in meteorology and climatology. Originally, such classifications—formerly known as synoptic type catalogs—were primarily developed for weather forecasting. Today, various classification methods are widely applied in many areas of atmospheric science for different purposes. Classification thus constitutes one of the core components of synoptic climatology [8]. These classifications provide a valuable analytical framework for evaluating both past and future climate variability. In particular, they help isolate the dynamic components of climate, i.e., changes in the frequency, persistence, or configuration of circulation types within multidecadal fluctuations and trends of atmospheric conditions [14]. Furthermore, they are widely used tools for describing and analyzing weather situations and climate regimes, offering a synthetic interpretation of complex synoptic processes [15].

The importance of classifying weather patterns has emerged significantly in recent decades, particularly in the analysis of air quality. Several studies have established a direct link between dominant synoptic systems and air pollution; for instance, Ref. [16] demonstrated that among five typical patterns in China's Yangtze River Delta, two specific circulation modes (Patterns 1 and 3) facilitate the transport of pollutants from other regions toward the Delta basin due to strong northwesterly winds. Consequently, synoptic maps serve as a predictive tool for air pollution trajectories [17]. This relationship is further refined using models that correlate wind direction and speed with pollutant concentrations, such as the Non-parametric Wind Regression (NWR) model used to classify meteorological impacts on impurity levels [18], or the Hybrid Single-Particle Lagrangian Integrated Trajectory (HYSPLIT) model, which enables real-time tracking of anthropogenic pollutant transport and sources [18]. Given the critical role of atmospheric circulation in driving extreme events, similar research has focused on linking specific circulation patterns to cold spells [19,20], heatwaves [21,22], and extreme precipitation [23].

In Morocco, earlier research has primarily focused on the relationship between large-scale atmospheric circulation modes—especially teleconnections—and certain climatic parameters, particularly precipitation. For instance, the relationship between characteristic mid-latitude weather regimes and precipitation in Morocco has been extensively studied [24]. Connections have also been established between the North Atlantic Oscillation (NAO) and various associated circulation types [25–29], as well as between the NAO and the Southern Oscillation [30]. The interaction between tropical and extratropical latitudes has also been explored [31–33]. However, studies on regional or sub-synoptic circulation regimes remain limited. Notably, Ref. [34] analyzed the southern slopes of the Atlas Mountains using output from the ECHAM4/OPYC3 and ECHAM5/MPI-OM1 climate models, focusing on precipitation. Similarly, Ref. [35] investigated typical weather types in Rabat, while Ref. [36] proposed a typology of summer weather situations. Other contributions, such as those by [37,38], have addressed precipitation variability. It is important to note that most studies on weather regimes in Morocco have concentrated on the effects of atmospheric circulation teleconnections (notably the NAO) or on specific synoptic events, often neglecting a detailed analysis of atmospheric circulation directly over Moroccan territory. Moreover, such research tends to be sectoral, limited to effects over a particular season or a restricted geographic area. As one exception, a focus on the mean surface circulation by integrating sea level pressure, maritime and continental trade winds, air temperature, and sea surface temperature (SST), enabled the characterization of the climatic break of the 1970s in Morocco and Mauritania. This analysis highlighted a strong increase in atmospheric pressure over the Mediterranean basin [39]. To bridge this research gap, the present study provides a comprehensive analysis of regional atmospheric circulation over Morocco, aiming to enhance the existing body of knowledge in this field of climate studies.

In this study, we aim to analyze the main components of regional atmospheric circulation around Morocco using principal component analysis (PCA) in its spatial form (S-mode) with Varimax rotation. To this end, we use the SynoptReg package, developed in R (version 4.4.2)R by [40], which allows for the extraction of dominant circulation regimes, the study of their monthly frequency, and the evaluation of their statistical trends. The study relies on data from the NCEP-DOE Reanalysis 2, including sea-level pressure (MSLP) and 500 hPa geopotential height (Z500) fields, with a spatial resolution of 2.5° in both latitude and longitude.

The article is structured into two main sections: the first presents the data used and the methodology adopted for classifying circulation types; the second is devoted to the analysis and discussion of the results, comparing them with findings from previous studies conducted in Morocco and neighboring regions.

2. Materials and Methods

2.1. Materials (Study Area and Data)

2.1.1. Study Area

Morocco (21–36° N, 1–17° W) is characterized by a unique geographical positioning that subjects it to diverse maritime influences from both the Atlantic Ocean and the Mediterranean Sea, as well as Saharan and orographic factors (Figure 1). According to the Köppen climate classification [41,42], four major climatic zones are identified: the Mediterranean climate (Cs) spanning the northern half of the country, the semi-arid steppe climate (BS) in the Eastern region (Oriental), the arid desert climate (BW) dominating the south and southeast, and the mountain Mediterranean climate (Ds). Geographically, Morocco serves as a critical junction for the interaction between polar air masses from the north and tropical air masses from the south.

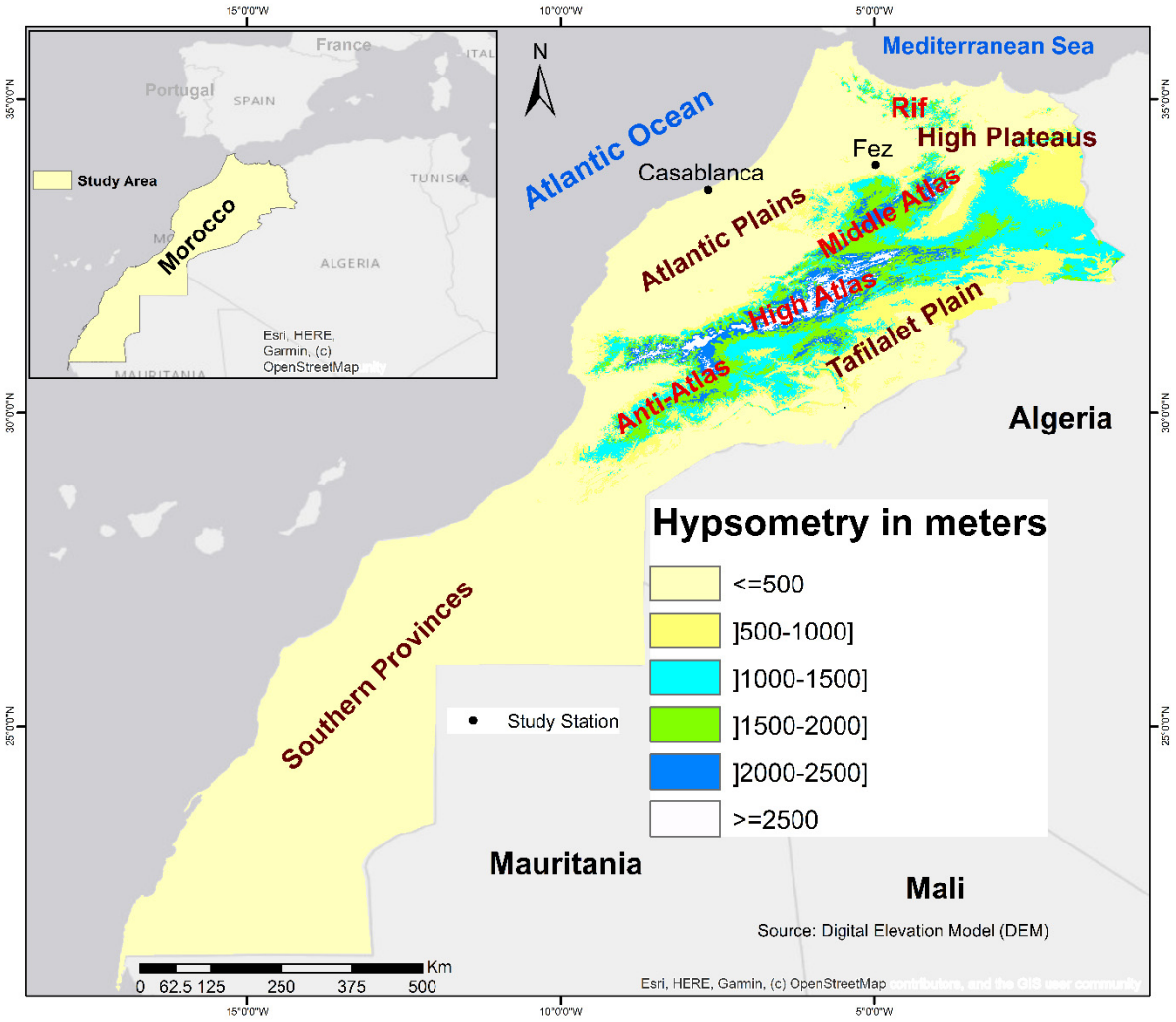

Figure 1. Geographical Setting and Main Orographic Features of Morocco.

2.1.2. NCEP Reanalysis Data: MSLP and Z500 Fields

This study is based on the NCEP-DOE Reanalysis II (R-2) model, produced by the National Centers for Environmental Prediction (NCEP). As detailed by [43], the R-2 model was specifically developed to resolve various errors and systematic biases identified in its predecessor. This model utilizes a sophisticated data assimilation system to integrate a wide array of observational sources—including satellite radiances, radiosondes, and surface reports—into a physically consistent global grid. Significant technical improvements in the R-2 version, such as the implementation of the Hong-Pan non-local boundary layer diffusion and the Chou shortwave radiation scheme, have enabled a more precise representation of tropospheric humidity and surface energy fluxes. Furthermore, the correction of the 'spectral snow' issue and the inclusion of a simple precipitation assimilation over land surfaces ensure that the Mean Sea Level Pressure (MSLP) and 500 hPa Geopotential Height (Z500) fields are homogenized and reliable for synoptic-scale analysis over Morocco. These data, provided at a spatial resolution of 2.5° × 2.5°, were obtained from the NOAA Physical Sciences Laboratory (PSL) and are publicly accessible (https://psl.noaa.gov/data/gridded/data.ncep.reanalysis2.html, accessed on 28 December 2024).

While Morocco's terrestrial boundaries extend from 21° N to 36° N and 1° W to 17° W, a synoptic domain of 20° to 40° N and 10° to 22.5° W was deliberately selected for this study. This extension is essential for tracking the dynamics of the primary atmospheric

centers of action, namely the Azores High, the Saharan thermal low, and the cyclonic disturbances associated with mid-latitude perturbations, all of which directly influence the Moroccan climate. By covering 126 grid points, this domain facilitates a full identification of regional Circulation Weather Types (CWTs) at both the sea level and the 500 hPa isobaric surface. This approach captures the daily variations in regional atmospheric circulation under the influence of the governing centers of action. To ensure a robust characterization, we employed a dual-parameter approach: while MSLP identifies surface-level pressure centers, the 500 hPa level represents geostrophic flows in the mid-troposphere and the passage of upper-level troughs and ridges, which mark polar and tropical influences, respectively. This integrated analysis of the tropospheric vertical structure is fundamental for understanding synoptic forcing across the Mediterranean and North African regions.

2.2. Methodology for CWT Classification and Synoptic Linkage to Extremes

In this study, we employed the PCA method applied in S-mode with Varimax rotation, using the SynoptReg package developed by [40]. This analytical mode is based on a data matrix where the variables correspond to grid points (MSLP and Z500), and the observations represent the days of the study period.

The application of S-mode PCA facilitates the removal of the spatial mean [25] and the identification of homogeneous variability zones, thereby enhancing the robustness of the results. Moreover, performing PCA without rotation can lead to instability in the factor subspace, limiting the interpretability of the findings. While this is a known challenge in climatology [26], it is equally relevant in broader environmental sciences; for instance, in air pollution research, where such methodology is essential for accurate source identification [44]. As a result, many researchers recommend the application of an orthogonal rotation—specifically Varimax rotation—to enhance the clarity and physical interpretability of the components.

Varimax rotation applied to the component matrix facilitates the identification of subgroups of grid points with similar temporal behavior [45]. This method aims to maximize the variance of the loadings within each principal component (PC), making the associated spatial structures more distinct. This facilitates the identification of well-defined CWT patterns while minimizing dependence on the initial spatial configuration. The spatial patterns obtained from the rotated PCs are generally more interpretable than those resulting from unrotated PCA [46,47]. After rotation, the principal components are ranked according to the percentage of variance explained in the study domain to isolate representative circulation types.

The extracted Principal Components (PCs), considering both their positive and negative phases, are interpreted as potential groups of Circulation Weather Types (CWTs). Following the methodological framework of [48], a threshold of ± 2 was applied to each component to identify the most representative synoptic days. Observations with extreme scores (greater than +2 or less than -2) were selected, as these extreme values characterize the most distinct atmospheric states within each component. The mean of these extreme days constitutes the centroids used for the subsequent K-means classification step.

Final classification is performed using the K-means method, using these centroids as initial seed points. Each day is then assigned to the group of CWT it is closest to. Previous studies have highlighted the usefulness of this approach in obtaining balanced groups [48,49]. This method is based on minimizing intra-cluster dispersion, which improves the internal cohesion of the groups [50].

The combined PCA—Varimax rotation and K-means classification approach thus provides a coherent, robust, and physically interpretable typology of CWT in the study region.

An analysis of the frequency of the extracted PCs was conducted at both annual and monthly time scales to examine their seasonal distribution and interannual variability. Subsequently, a trend analysis of the annual frequency of these components was carried out using a linear regression model applied to the time series of each PC frequency. The statistical significance of these trends was assessed using the *p*-values associated with the slope coefficients, allowing us to identify the components whose evolution is statistically significant at confidence levels between 0.1 and 0.01.

To evaluate the relationship between atmospheric circulation and extreme meteorological events, a rigorous synchronization procedure was established between the daily CWT catalog and ground-based observations provided by the General Directorate of Meteorology (DGM, Casablanca Morocco). The identification of extreme thermal events followed a percentile-based methodology, as recommended by [51]. A heatwave was defined as a period of at least three consecutive days where both maximum and minimum temperatures (Tmax and Tmin) reached or exceeded the 9th decile (90th percentile). This analysis specifically focused on the summer months, characterized by significantly higher temperature thresholds compared to other seasons. Regarding precipitation, events were classified as 'wet days' using a daily threshold of $\geq$1 mm, in strict adherence to the international standards established by the Expert Team on Climate Change Detection and Indices (ETCCDI) and implemented within the Climpact framework (https://climpact-sci.org/). By cross-referencing these standardized extreme event dates with the synchronized daily atmospheric circulations, we calculated the percentage contribution of each Circulation Weather Type (CWT) at both the Sea Level Pressure (SLP) and the 500 hPa geopotential height (z500) levels.

3. Results and Discussion

3.1. Representative PCs of Surface CWTs (MSLP in hPa)

The selection of six clusters was primarily dictated by their ability to encapsulate the diverse atmospheric circulation patterns affecting Morocco. Statistically, the first six principal components (PCs) account for 95% of the total variance (see Supplementary Materials, Figure S1 and Table S1), providing a robust representation of atmospheric variability while filtering out residual statistical noise. To validate this selection, the K-means clustering method was applied to these PCs, confirming that six clusters achieve an optimal balance between granularity and redundancy. Physically, this number (k = 6) allows for a clear distinction between key synoptic configurations affecting the region, notably Atlantic disturbances, Saharan thermal lows, and the varying positions of the Azores High, without over-segmenting the data into overlapping or non-significant patterns. Furthermore, although 5% of the initial variance was excluded as noise, the clustering procedure effectively reassigned all study days to their most statistically similar synoptic type. Consequently, the annual frequencies presented in Table 1 reflect the comprehensive daily contribution of each pattern, ensuring that no meteorological cases were omitted from the final analysis.

Table 1. Annual relative frequency of PC at Mean Sea Level Pressure (MSLP) (1980–2019).

	PC 1	PC 2	PC 3	PC 4	PC 5	PC 6
Frequency of days (%)	10.10	35.00	13.31	11.50	13.79	16.3

Each component was analyzed in both its positive and negative phases, following the functionalities of the SynoptReg package [40]. As a result, three initially extracted components yielded six distinct PC groups, enabling a nuanced interpretation of the CWT observed during the study period (Figure 2).

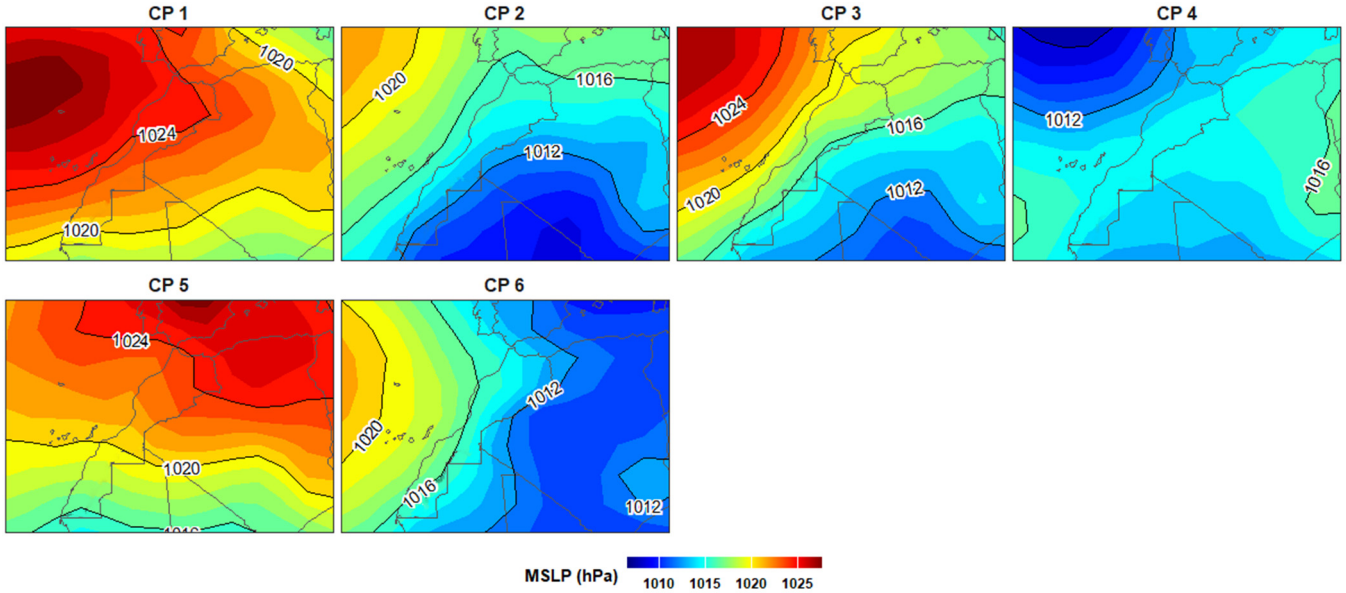

Figure 2. Spatial patterns of the Circulation Weather Types (CWT) in terms of Mean Sea Level Pressure (MSLP).

PC1 reflects an extension of the Azores anticyclonic ridge toward Morocco, dynamically driven by the descending branch of the Hadley Cell over the tropical regions of the Northern Hemisphere. This configuration corresponds to an anticyclonic circulation type, typically associated with stable atmospheric conditions that inhibit the intrusion of polar frontal disturbances.

PC2 corresponds to the development of a thermally induced low-pressure system, with its center (1009 hPa) located over northern Mali, while the Azores High retracts toward the central Atlantic Ocean. This configuration aligns with several studies examining the relationship between the Saharan low-pressure system and mid-latitude circulations [52–55]. It represents a cyclonic circulation type, generally associated with hot and dry weather conditions during the summer season [55]. Moreover, Ref. [56] showed that the northward shift in the Saharan low-pressure system is strongly correlated with a maximum in solar radiation transfer toward northern regions, confirming its thermal origin.

PC3 illustrates an intermediate configuration between those described by PC1 and PC2. In this case, the Azores High is positioned closer to the Moroccan coast, while the Saharan low adopts a more southerly position compared to PC2. This specific placement of pressure systems around the territory promotes a northeast (NE) circulation, whose increased winter frequency is generally associated with cold and dry conditions in Morocco. Conversely, during the summer season, this same configuration is often responsible for intense heatwaves across the country [55].

PC4 highlights the presence of a depression system centered off the Portuguese coast. This is a dynamically driven depression typical of temperate latitudes, linked to the proximity of the polar front in the Iberian-Atlantic and Moroccan regions. This configuration is favored by a southerly position of the Azores High, which allows the incursion of disturbed westerly flows into Morocco. This type of cyclonic circulation supports the arrival of precipitation in the country due to the advection of moist air masses from the west (W), northwest (NW), and southwest (SW) sectors [55].

PC5 represents an atmospheric configuration characterized by a northward extension of the subtropical high-pressure system, covering the Iberian Peninsula and the western Mediterranean basin, while the Saharan depression remains more southerly. The fifth component represents a situation of the subtropical high pressure over the Iberian Peninsula

and the western Mediterranean Sea, a situation confirmed by a recent study on Spanish territory [57].

Finally, PC6 depicts a progressive decrease in atmospheric pressure from the west, consistent with [58] findings on atmospheric dynamics in the western Mediterranean basin. This configuration favors the establishment of a northerly circulation over Morocco, characterized by the advection of cool and moist air masses from the North Atlantic, significantly influencing winter and spring weather conditions in the region (see Table 2).

Table 2. Percentage contribution (%) of NCEP-DOE Reanalysis II Principal Components (Sea Level) to heatwaves and precipitation events, derived from raw data provided by the General Directorate of Meteorology (DGM, Morocco).

Rainfall		Heatwaves		Phenomenon
≥1 mm		≥90th Percentile for 3 Consecutive Days (Tmax & Tmin) During Summer		Statistical Threshold
Fez	Casablanca	Fez	Casablanca	Station
12.71	11.33	0	0	PC 1
8.17	13.46	98.63	98.87	PC 2
4.49	5.51	1.37	1.13	PC 3
30.07	24.84	0	0	PC 4
4.66	4.57	0	0	PC 5
39.91	40.29	0	0	PC 6

On an annual scale, the relative frequency of the components highlights the dominance of PC2, while the other components display relatively similar annual frequencies (Table 1). It is also useful to analyze the relative frequency of each component according to the different months of the year.

- Monthly analysis of the frequencies of PC of CWTs at the Mean Sea Level Pressure (MSLP)

The monthly analysis of the principal components reveals that the frequency of PC1 is particularly high during the winter months (December, January, and February). This component is associated with the extension of the Azores anticyclonic ridge over Moroccan territory, which is further reinforced by snow cover over the Atlas Mountains during this season [38]. Its frequency peaks in January at 36%, followed by December at 28% (Figure 3). A study by [59] on the western Mediterranean showed that this situation experienced a notable increase in winter between 1979 and 2009, compared to other seasons. Furthermore, Ref. [60] demonstrated that the expansion of the Azores High began as early as 1850 and has intensified significantly throughout the twentieth century. Similarly, Ref. [61] highlighted a strengthening of extreme configurations of the subtropical anticyclone during winter in the western Mediterranean.

This is followed by the fifth principal component (PC5), which corresponds to an atmospheric pattern characterized by anticyclonic circulation, predominantly resulting in dry weather conditions over Morocco (Table 2). This weather regime was also identified by [62] in their analysis of Mediterranean weather patterns. It mainly occurs between October and March, with a peak frequency in December.

PC4 contributes significantly to atmospheric circulation from October (18.4%) to December (15.2%) and to a lesser extent in March. It corresponds to a configuration characterized by local cyclogenesis influenced by disturbances originating from temperate latitudes. These disturbances, responsible for local depressions in several Mediterranean

regions, including Morocco (Table 2), occur when mid-latitude low-pressure systems interact with the upper-level jet stream, which reaches its southernmost position [63].

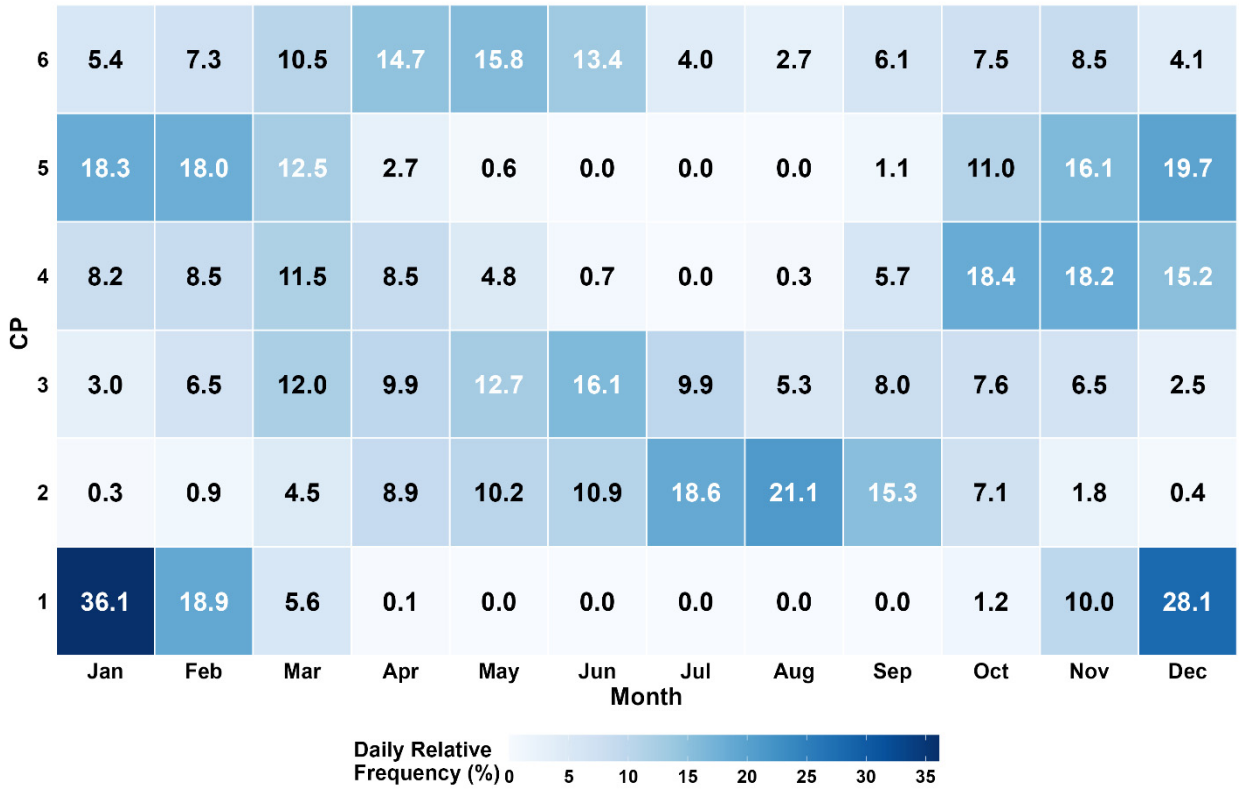

Figure 3. Monthly relative frequencies of PC of Surface CWT.

During the winter season, it has been recently demonstrated that PC1 and PC5 are the dominant configurations [57,64]. Other principal components contribute relatively little during this period. In winter, the Saharan depression tends to almost completely disappear from northern Africa, retreating southward beyond the Darfur Mountains, as shown by the work of [56].

PC6, representing a northerly advective flow, is more frequent between March and June (Figures 2 and 3). The atmospheric configuration associated with this component marks a transition phase toward northeasterly and easterly circulations, as confirmed by previous studies [64]. This situation could result from the combined intensification of Afro-Asian depressions and the subtropical anticyclone, which become characteristic of much of the Mediterranean basin during spring [63].

The period from March to July is marked by a higher frequency of PC3, while the April–September season is dominated by PC2 (21.1% in August). Both components correspond to an atmospheric configuration characterized by a northeasterly (NE) flow over Morocco. This flow is particularly pronounced in the case of PC3 due to a steeper pressure gradient associated with this configuration. During this time of year—spanning from spring to early autumn—dominated by hot and dry conditions, there is a marked retreat of the subtropical anticyclone toward the central Atlantic Ocean, between 30° and 50° N and 20° to 50° W [65].

In the Mediterranean context, this westward retreat of the subtropical anticyclone has also been documented, coinciding with a northward extension of the Saharan depression [58]. This retreat of the Azores High toward western Morocco promotes the expansion of the Saharan depression between the Hoggar and Atlas Mountains [56,64], thus leading to a significant rise in temperatures across North Africa and the Mediterranean basin [66].

In July, the subtropical anticyclone reaches its maximum intensity over the heart of the North Atlantic Ocean [67], facilitating the sustained establishment of NE and E flows over Moroccan territory. As a result, PC2 and PC3 become the most frequent during this period (Figure 3).

The monthly frequency analysis shows that PC1 is predominantly observed during the calendar months of the rainy season (December 28.1%, January 36.1%). However, it is essential to clarify that PC1 represents an anticyclonic configuration. Its high frequency during this period does not imply precipitation; on the contrary, it accounts for the persistence of stable conditions and dry spells within the wet season, as the region remains under the influence of the Azores High.

Furthermore, PC4 and PC5 are almost entirely absent during the summer season. PC4, linked to cyclogenesis processes, generates unstable weather conducive to precipitation. In contrast, PC5 is associated with an easterly to southeasterly flow, often responsible for dry conditions. This configuration may lead to reduced precipitation due to the extension of high pressure over the Mediterranean and North Africa 32. Conversely, PC3 and PC6 occur throughout the year. PC3 frequency peaks in June (16.1%), while PC6 peaks in April (14.7%) and May (15.8%). These configurations reflect the seasonal variability of CWT regimes over Morocco and illustrate the contrasts between wet and dry seasons through their differing occurrences.

- Trend analysis of the PCs representative of CWTs at the Mean Sea Level Pressure (MSLP)

Following the frequency analysis of the PCs at both annual and monthly scales, it is relevant to examine the trends of these components over the 1980–2019 period. The results of this analysis (Figure 4) reveal that only PC2 and PC3 exhibit statistically significant trends, and in opposite directions.

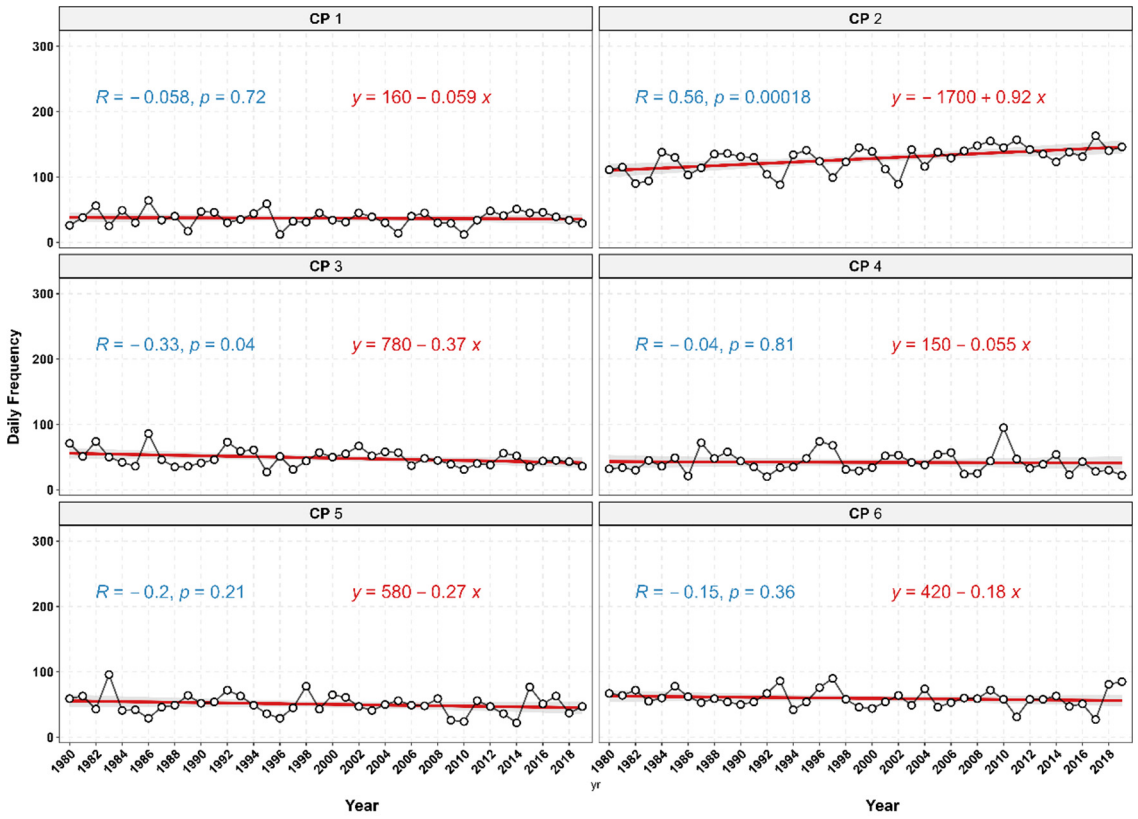

Figure 4. Annual trends of 6 PCs of surface CWTs (MSLP). White Circles: Annual observations (data points). Red Line & Equation: Linear regression trend and its formula. Grey Area: 95% Confidence Interval. Blue Statistics: Pearson correlation (R) and p-value.

PC2 shows a highly significant upward trend at the 0.01 level ($p = 1.8 \times 10^{-4}$), whereas PC3 displays a significant downward trend at the 0.05 level ($p = 0.04$). It is worth noting that both components are associated with northeastern to anticyclonic northeastern circulation regimes, according to the Lamb classification [55]. However, their atmospheric characteristics differ substantially.

PC2 is linked to a strengthening of the Saharan low, which tends to shift northward, along with a weakening of the pressure gradient associated with the Azores High. In contrast, PC3 reflects a situation in which the Saharan depression is located further south, with a stronger pressure gradient between it and the Azores anticyclone. These two contrasting configurations reflect an overall trend toward the intensification and northward extension of the Saharan low, accompanied by a gradual weakening of the Azores High.

The reduction in the pressure gradient observed in the configuration associated with PC2 suggests a decrease in northeasterly wind speeds. This observation aligns with the findings of [64], who reported a decline in mean wind speed due to the weakening of the pressure gradient within the Azores High, particularly during summer and autumn, by the end of the 21st century. They also highlighted a significant increase in the frequency of thermal lows over the greater Sahara and the Iberian Peninsula. These elements confirm the increasing trend of PC2 frequency over Morocco observed in the present study.

The increased frequency of PC2 may also contribute to the intensification of heatwaves in the study region (Table 2). These results are consistent with those of [68] for Spain and [57] for the Iberian Atlantic coast. Furthermore, Ref. [68] identified a positive trend in dry weather regimes alongside a negative trend in westerly regimes, which are typically associated with a high probability of precipitation, an evolution also observed in Morocco by [30].

To consolidate these results, we conduct a Principal Component Analysis (PCA) of the circulation at the 500 hPa isobaric surface. The objective is to investigate the role of ridges and troughs within the mid-troposphere and to examine the extent to which their evolution is in phase with the atmospheric circulation patterns observed at sea level.

3.2. Representative PCs of CWTs at the 500 hPa Isobaric Level (Geopotential Decameters (dam))

While the Principal Component Analysis (PCA) of atmospheric circulation at sea level is essential for identifying the locations of surface anticyclones and depressions, the classification based on the 500 hPa isobaric surface provides an understanding of mid-tropospheric dynamics. This S-mode PCA-based classification extracts six principal components that describe the geopotential height at this level. These six PCs account for 97% of the total daily variability prior to rotation (see Supplementary Materials, Figure S2 and Table S2). Following the same methodological steps applied at the surface level—including Varimax rotation and K-means clustering—these components effectively cover 100% of the study days. This ensures that every daily observation is assigned to its most statistically similar mid-tropospheric pattern, allowing for a direct correlation between surface-level trends and the atmospheric dynamics at this altitude.

The PCA of CWTs reveals six principal components (PCs). Overall, PC1 is the most frequent, with a frequency reaching 23%, followed by PC3, while the remaining principal components show relatively low and comparable frequencies (Table 3).

Table 3. Annual relative frequency of the representative PCs of the CWTs at the 500 hPa level during the period 1980–2019.

	PC 1	**PC 2**	**PC 3**	**PC 4**	**PC 5**	**PC 6**
Frequency of days (%)	22.69	14.59	20.27	13.51	15.85	13.09

The atmospheric configurations described by the geopotential heights of the 500 hPa isobaric surface (in decameters geopotential—dam) are relatively simple, generally taking the form of troughs or ridges, yet they show important nuances. Low geopotential heights, corresponding to surface low-pressure zones, are located below 556 dam, while high geopotential heights, associated with surface high-pressure zones, exceed this threshold.

According to the first component, it appears that the Moroccan territory lies within an area characterized by high isobaric levels, particularly in the Southern and South-Eastern regions (Figure 5). The meteorological situation takes the form of a quasi-zonal flow regime, with a Southwest/Northeast axis.

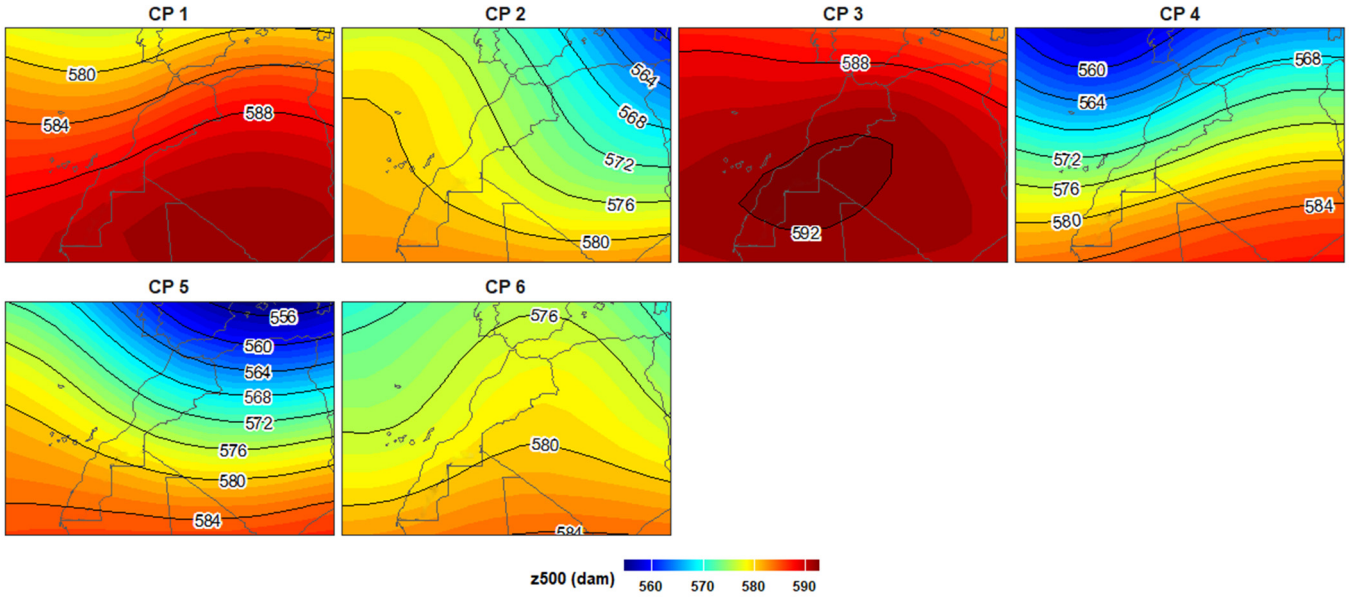

Figure 5. Spatial patterns of the Circulation Weather Types (CWT) for the 500 hPa geopotential height, expressed in geopotential decameters (dam).

The second component shows Morocco in a transition zone between troughs and ridges in the middle tropospheric layers, with troughs located to the East and Northeast, and ridges to the South and Southwest.

The third component represents a ridge directly over Moroccan territory, corresponding to the Southern regions being at high isobaric levels. The first and third components primarily contribute to the arrival of warm air masses towards Morocco (Table 4). The characteristic meteorological situation at this isobaric level blocks the upward processes of warm air from the surface to the middle and upper layers. This is due to lower temperatures in the center of the troposphere over North Africa, which slows the upward movements of warm air [69]. Furthermore, the situation where the Saharan low exhibits high temperatures to the West and lower temperatures to the East strongly influences rising temperatures in North and West Africa [53]. This leads to surface-level circulations from the East and Northeast, often resulting in temperatures in North Africa rising beyond usual values.

The fourth and fifth components (Figure 5) show a zonal gradient of isobaric surfaces from north to south, with differences in the intensity of this gradient between the two components. In the fourth component, the zone of strongest descent in the isobaric surfaces appears in Northwestern Morocco, while the area of strongest ascent is in the Southeastern part of the country. Conversely, the fifth component shows that the zone of strongest descent manifests in Northeastern Morocco, whereas the ascent is located in the Southwest.

Table 4. Contribution (%) of NCEP-DOE Reanalysis II Principal Components (500 hPa) to heatwaves and precipitation events, derived from raw data provided by the General Directorate of Meteorology (DGM, Morocco).

Precipitation		Heatwaves		Phenomenon
≥1 mm (1980–2016)		≥90th Percentile for 3 Consecutive Days (Tmax & Tmin) During Summer (1980–2019)		Statistical Threshold
Fes	Casablanca	Fes	Casablanca	Station
11.72	7.65	24.42	20.46	PC 1
6.66	7.42	0	0	PC 2
2.09	0.69	74.42	77.27	PC 3
33.04	36.28	0	0	PC 4
42.57	43.76	0	0	PC 5
3.92	4.2	1.16	2.27	PC 6

Additionally, the fourth component corresponds to a situation where the semi-polar jet stream emerges in the upper atmospheric layers, allowing disturbances to reach Morocco. The fifth component, on the other hand, shows the entry situation of this jet stream, typically leading to an absence of disturbances in the country. In this situation, Morocco lies within areas characterized by descending air from the upper layers.

The last component is distinguished by a weak gradient of isobaric surfaces over Morocco compared to the other components and does not present any clearly identifiable meteorological configuration.

- Monthly analysis of the frequencies of PC of CWTs at the 500 hPa isobaric surface

The monthly relative frequency of PCs clearly distinguishes those associated with the hot and dry season from those typical of the wet season (Figure 6). Indeed, PC1 and PC3 characterize the months from May to October and from June to October, respectively. These components correspond to ridges associated with tropical warm air advection, responsible for the establishment of strong high geopotential over the country. The frequency of PC1 peaks in June (24.5%), while that of PC3 reaches its maximum in July (27.7%) and August (28.1%). These two atmospheric configurations lead to a high frequency of heatwaves in Morocco, with the third component (PC3) showing the most significant impact during the peak summer months (Table 4).

Conversely, the other components, mainly associated with the wet season, are mostly related to upper-level troughs, with the exception of PC6, which also represents a high-pressure system but is less pronounced than PC1 and PC3. The frequency of these wet-season components is higher between November and April, the wettest period of the year.

According to [69], these synoptic conditions are accompanied by inversion layers in the lower troposphere, characteristic of the hot Saharan depression in summer. This is an aerological situation dominated by warm air both at the surface and in the upper levels. The appearance of such configurations is generally followed by hot and dry weather at the surface, due to the northward shift in the Saharan low-pressure system beyond its usual position, along with the advection of tropical warm air aloft.

Regarding the components associated with the rainy season, it has been established that the passage of upper-level troughs, a result of slow atmospheric circulation, plays a crucial role in the formation of precipitation over Morocco. Processes of convective instability and dynamic ascent typically develop to the east and beneath the axes of these troughs. This is exemplified by PC4, where such conditions can induce cyclogenesis, leading to rainfall across much of Atlantic Morocco and its mountainous regions (Table 4).

Precipitation is also linked to the characteristic pattern of PC5 (Table 4); however, it remains generally weak. This is because the associated upper-level troughs are typically positioned or deepen to the east of the Moroccan domain.

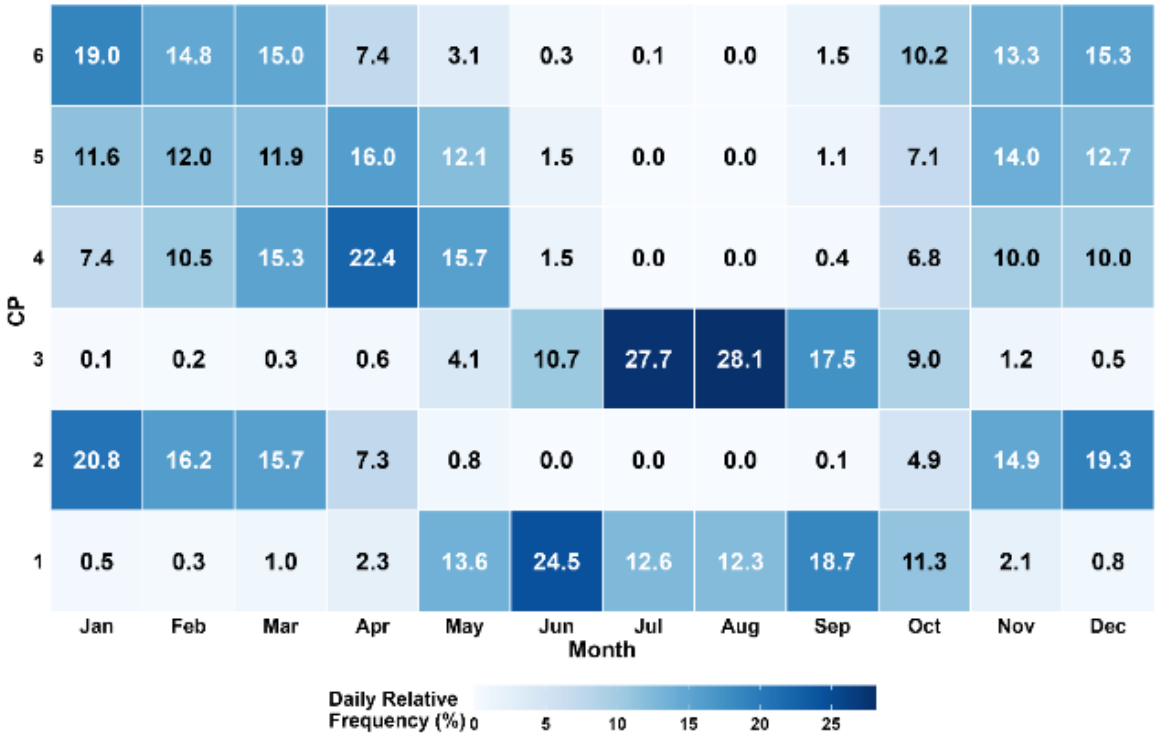

Figure 6. Monthly frequency of the PCs representative of CWTs at the 500 hPa level.

In contrast, along the Mediterranean coast, most precipitation is observed on the western side of the upper-level trough (as in PC2) [33], where cyclogenesis often occurs over the western Mediterranean Sea.

In the Anti-Atlas region, precipitation events are associated with deep troughs extending as far as the Canary Islands or the Sahara (e.g., PC4). These events typically occur east of the trough axis [33], with the orographic effect of the High Atlas further enhancing precipitation.

When the upper-level troughs deepen significantly, they may trigger local cyclogenesis. In extreme cases of meridional cold polar air advection aloft, a cold cut-off low may detach from the main flow and settle within the subtropical warm air mass that dominates the upper troposphere above Morocco. This configuration generates strong convective instability, potentially causing heavy precipitation over large areas of the country [55].

Such local depressions [65,70] explain the occurrence of precipitation, especially in regions shielded from the direct influence of Atlantic lows thanks to the presence of orographic barriers such as the southern slopes of the Atlas Mountains and the Mediterranean coast.

This monthly frequency analysis of principal components, which represent mid-tropospheric atmospheric configurations, highlights a strong coherence between seasonal characteristics and dominant atmospheric patterns. It therefore becomes essential to examine the annual trends of these components in order to identify those most affected by climate change. This approach will also allow for assessing the extent to which these evolutions align with trends observed in the principal components characterizing surface atmospheric circulation.

- Trend analysis of the PCs representative of CWTs at the 500 hPa isobaric surface altitude levels (dam)

The trend analysis of the principal components (PCs) revealed that five of the six identified components exhibited statistically significant trends during the study period. Specifically, components PC3 and PC5 showed a significant increasing trend at the 95% confidence level. In contrast, components PC2 (at the 95% level), PC4, and PC6 (at the 90% level) displayed a significant decreasing trend, as illustrated in Figure 7.

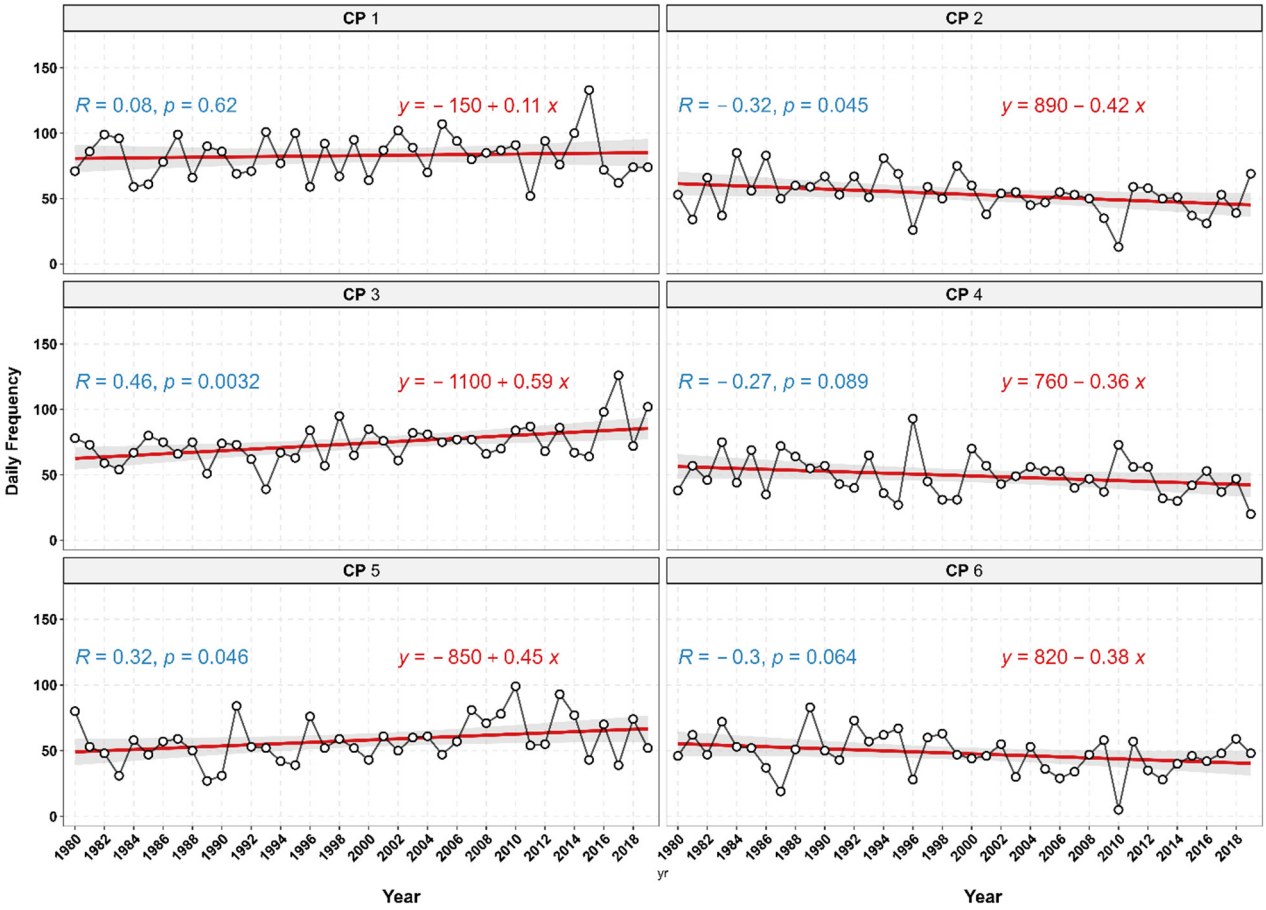

Figure 7. Annual trends of PCs representative of the CWTs at the 500 hPa isobaric surface level. White circles represent annual observations, the red line shows the linear regression trend, and the grey area indicates the 95% confidence interval.

The positive trend in PC3 reflects an increasing frequency of ridging (upper-level high pressure) in the mid-troposphere. This pattern is likely to lead to a higher frequency of hot and dry weather conditions during the warm season in Morocco, as it is associated, at sea level, with the northward advance of the Saharan thermal low, which facilitates the advection of hot, dry air masses with an easterly to northeasterly flow.

Conversely, the increase in PC5 is linked to a low probability of rainy days, as it represents a scenario where the Moroccan region lies within the exit region of the upper-level jet stream—a synoptic pattern typically not conducive to precipitation over Morocco.

The decline in the frequency of PC2 and PC6 corresponds to a decrease in the occurrence of thermally mild and dry weather. This is because these components are associated with the prevalence of high-pressure systems over the Moroccan region, albeit of weaker intensity.

Meanwhile, PC4 exhibits a negative trend, which may result in a decrease in wet days. This component represents patterns associated with the deepening and passage of

synoptic-scale low-pressure systems (disturbances) across northern Morocco, particularly its northwestern face.

Collectively, the observed decline in these key atmospheric circulation components suggests a potential future increase in the frequency of warmer weather patterns.

Previous studies have shown that the decline in precipitation over the southern Mediterranean basin is related to a decrease in the frequency of atmospheric depressions affecting the southern shore, contrasted with an increase in their occurrence over the northern shore [71]. This evolution is largely attributed to a shift in depression tracks, deviated northward [25]. The retreat of these low-pressure systems may be linked to the gradual displacement of the baroclinic zone toward higher latitudes [25], thereby favoring the prolonged persistence of high-pressure systems over North Africa. Furthermore, multiple studies have demonstrated that the subtropical anticyclone has shifted northward since the 1970s, thereby enhancing the blocking of perturbation flows from mid-latitudes [72].

The components showing statistically significant increases are associated with ridge configurations over Moroccan territory, indicating a higher likelihood of hot days, particularly during summer months when these patterns are most frequent. Previous synoptic-scale studies have highlighted a northward and northeastward shift in circulation at mid-tropospheric levels. This shift is manifested by an increased concentration of isobaric levels above Morocco and southwestern Europe [26,73], a rise in the frequency of the zonal phase of the North Atlantic Oscillation (NAO) [74,75], as well as the expansion of the subtropical anticyclone [60]. Additionally, an increase in the frequency of easterly circulations, at the expense of westerly circulations, has been observed [25], reinforcing the warm and dry nature of dominant weather patterns in Morocco over recent decades.

4. Limitations and Directions for Future Research

Despite the results obtained in this study, which reveal a trend towards an increased frequency of dry and hot air masses during the hot season and an increased frequency of anticyclonic situations during the rainy season (based on the NCEP-DOE Reanalysis II model), these findings require cautious interpretation, taking into account the following methodological limitations:

Firstly, this study relied on a single modeling data source. To enhance the robustness and generalizability of the results, it is recommended to replicate the analysis using additional data sources, such as ERA5 reanalysis data. This would allow for a test of the findings' consistency across different datasets, including those with higher spatial resolutions. It is expected, however, that the regional atmospheric circulation patterns and trends studied here will be fairly uniform across reanalyses.

Secondly, the analysis remained at the regional scale, without exploring potential correlative or causal relationships with large-scale climate variability modes, such as the North Atlantic Oscillation (NAO), the Atlantic ridge regime, and atmospheric blocking. Integrating such cross-scale analysis into future research would help distinguish local influences from those related to synoptic-scale atmospheric circulation.

Thirdly, the study focused on analyzing the characteristics of the classified circulation weather types themselves, without extending this analysis to evaluate their detailed impacts on key surface climate variables, particularly temperature and precipitation at the local scale. Bridging this gap between the analysis of atmospheric dynamics and its direct climatic effects constitutes a necessary avenue for future research, given its importance for climate change adaptation strategies.

5. Conclusions

This study is situated within the context of Morocco's increasing vulnerability to climate change, marked by a growing risk of heatwaves and prolonged droughts. It aims to analyze the variability and trends of CWTs at both surface and upper levels (Z500) over the period 1980–2019 in order to better understand the synoptic configurations influencing the regional climate. To this end, a classification of CWTs was performed using spatial PCA with Varimax rotation, applied to sea level pressure fields and 500 hPa geopotential height from the NCEP/DOE reanalysis dataset.

The surface-level analysis reveals strong seasonal variability as well as significant changes in dominant circulation regimes. Anticyclonic configurations, notably PC1, predominate in winter and reflect a stable atmospheric situation linked to the extension of the Azores high ridge. Conversely, PCs 2 and 3, dominant from spring to early autumn, are associated with northeast sector flows influenced by the variable position of the Azores high and the Saharan low. A marked increase in PC2 indicates a strengthening and northward progression of the Saharan low, as demonstrated by the study of [56]. This trend is further confirmed by more recent multi-model simulations [76], which show a significant intensification in Saharan Heat Low (SHL) activity during the 2000s compared to the 1980s. Conversely, the decline in PC3 reflects a strengthening of the Azores high combined with a more southerly position of the Saharan low. This trend towards a gradual northward shift in the Saharan low points to a transition toward conditions that exacerbate summer drought and increase the frequency and intensity of heatwaves during the same season in Morocco. This finding aligns with expected climate change impacts in the western Mediterranean basin. Ref. [77] highlighted an increase in the number of dry days in the Azores region as a result of the strengthening of this high-pressure system by the end of the 21st century.

At altitude, the analysis of circulation types at 500 hPa shows that ridges (PC1 and PC3), predominant in the warm season, correspond to a meridional south-to-north flow of warm tropical and continental air, reinforcing atmospheric stability and favoring a hot and dry climate during this part of the year. These conditions in the mid-troposphere during the dry season are reinforced by surface evolution characterized by a strengthening and northward displacement of the Saharan low. In contrast, upper-level troughs (PC4, PC5) and PC6—a less pronounced ridge extending south to north across Morocco—predominate during the wet season. The passage of these troughs over Morocco favors cyclogenesis and atmospheric instability. The significant decrease in the frequency of troughs, particularly PC4, reflects a retreat of conditions favorable to instability and precipitation, thus contributing to the recurrence of drought episodes during the normally rainy period from November to March.

In conclusion, the analysis of atmospheric dynamics over Morocco reveals a trend toward unfavorable climatic conditions during both the dry-hot and wet seasons. During the dry season, the aerological structure characterized by the establishment of warm continental tropical air at surface and upper levels promotes the strengthening of the Saharan low as well as the intensification of a strong geopotential high aloft. These phenomena contribute to the increase and intensification of the risk of summer heatwaves. Conversely, during the rainy season, the decline in the frequency of upper-level troughs—especially PC4, whose axis is located west of the country—may explain the recurrent drought episodes observed over the past four decades (1980–2019).

This evolution is consistent with current observations and future climate projections for the Mediterranean region and highlights the crucial importance of such diagnostics to effectively anticipate and better manage the impacts of climate change on water resources, agriculture, forest ecosystems, and the health of vulnerable populations.

Supplementary Materials: The following supporting information can be downloaded at: https://www.mdpi.com/article/10.3390/atmos17050445/s1, Figure S1: Proportion of total variance explained by the initial Principal Components (PCs) for Mean Sea Level Pressure (MSLP) (1980–2019); Figure S2: Proportion of total variance explained by the initial Principal Components (PCs) for the 500 hPa geopotential height (1980–2019); Table S1: Summary of Principal Component Analysis (PCA) for Surface Mean Sea Level Pressure (MSLP); Table S2: Summary of Principal Component Analysis (PCA) for the 500 hPa geopotential height.

Author Contributions: Conceptualization, J.E.K. and M.H.; methodology, J.E.K. and M.H.; software, J.E.K.; validation, N.Y.K., R.K. and M.H.; formal analysis, J.E.K.; investigation, J.E.K. and M.H.; resources, M.H.; data curation, R.K.; writing—original draft preparation J.E.K. and M.H.; writing—review and editing, J.E.K., M.H., N.Y.K., L.A. and R.K.; visualization, J.E.K.; supervision, M.H. and N.Y.K.; project administration, M.H. All authors have read and agreed to the published version of the manuscript.

Funding: This research received no external funding.

Institutional Review Board Statement: Not applicable.

Informed Consent Statement: Not applicable.

Data Availability Statement: The data presented in this study are available on request from the corresponding authors.

Conflicts of Interest: The authors declare no conflicts of interest.

References

1. Calvin, K.; Dasgupta, D.; Krinner, G.; Mukherji, A.; Thorne, P.W.; Trisos, C.; Romero, J.; Aldunce, P.; Barrett, K.; Blanco, G.; et al. *IPCC, 2023: Climate Change 2023: Synthesis Report. Contribution of Working Groups I, II and III to the Sixth Assessment Report of the Intergovernmental Panel on Climate Change*, 1st ed.; Core Writing Team, Lee, H., Romero, J., Eds.; IPCC: Geneva, Switzerland, 2023. [CrossRef]
2. Cherif, S.; Doblas-Miranda, E.; Lionello, P.; Borrego, C.; Giorgi, F.; Iglesias, A.; Jebari, S.; Mahmoudi, E.; Moriondo, M.; Pringault, O.; et al. Drivers of change. In *Climate and Environmental Change in the Mediterranean Basin—Current Situation and Risks for the Future*; First Mediterranean Assessment Report; Cramer, W., Guiot, J., Marini, K., Eds.; Union for the Mediterranean, Plan Bleu, UNEP/MAP: Marseille, France; pp. 59–180. [CrossRef]
3. Noto, L.V.; Cipolla, G.; Pumo, D.; Francipane, A. Climate Change in the Mediterranean Basin (Part II): A Review of Challenges and Uncertainties in Climate Change Modeling and Impact Analyses. *Water Resour. Manag.* **2023**, *37*, 2307–2323. [CrossRef]
4. Moreno, M.; Bertolín, C.; Arlanzón, D.; Ortiz, P.; Ortiz, R. Climate change, large fires, and cultural landscapes in the mediterranean basin: An analysis in southern Spain. *Heliyon* **2023**, *9*, e16941. [CrossRef] [PubMed]
5. Pérez-Cutillas, P.; Salhi, A. Long-term hydroclimatic projections and climate change scenarios at regional scale in Morocco. *J. Environ. Manag.* **2024**, *371*, 123254. [CrossRef]
6. Conway, D.; Jones, P.D. The use of weather types and air flow indices for GCM downscaling. *J. Hydrol.* **1998**, *212–213*, 348–361. [CrossRef]
7. El Kenawy, A.M.; Mccabe, M.F.; Stenchikov, G.L.; Raj, J. Multi-decadal classification of synoptic weather types, observed trends and links to rainfall characteristics over Saudi Arabia. *Front. Environ. Sci.* **2014**, *2*, 37. [CrossRef]
8. Huth, R.; Beck, C.; Philipp, A.; Demuzere, M.; Ustrnul, Z.; Cahynová, M.; Kyselý, J.; Tveito, O.E. Classifications of Atmospheric Circulation Patterns: Recent Advances and Applications. *Ann. N. Y. Acad. Sci.* **2008**, *1146*, 105–152. [CrossRef] [PubMed]
9. Vautard, R. Multiple Weather Regimes over the North Atlantic: Analysis of Precursors and Successors. *Mon. Weather. Rev.* **1990**, *118*, 2056–2081. [CrossRef]
10. Rodríguez, O.; Lemus-Canovas, M. Synoptic patterns triggering tornadic storms on the Iberian Peninsula and the Balearic Islands. *Atmos. Res.* **2023**, *285*, 106634. [CrossRef]
11. Bonsoms, J.; Oliva, M.; López-Moreno, J.I.; Fettweis, X. Rising Extreme Meltwater Trends in Greenland Ice Sheet (1950–2022): Surface Energy Balance and Large-Scale Circulation Changes. *J. Clim.* **2024**, *37*, 4851–4866. [CrossRef]
12. Sánchez-Almodóvar, E.; Martin-Vide, J.; Olcina-Cantos, J.; Lemus-Canovas, M. Are Atmospheric Situations Now More Favourable for Heavy Rainfall in the Spanish Mediterranean? Analysis of Episodes in the Alicante Province (1981–2020). *Atmosphere* **2022**, *13*, 1410. [CrossRef]

13. Jones, P.D.; Harpham, C.; Briffa, K.R. Lamb weather types derived from reanalysis products. *Int. J. Climatol.* **2013**, *33*, 1129–1139. [CrossRef]
14. Richardson, D.; Neal, R.; Dankers, R.; Mylne, K.; Cowling, R.; Clements, H.; Millard, J. Linking weather patterns to regional extreme precipitation for highlighting potential flood events in medium- to long-range forecasts. *Meteorol. Appl.* **2020**, *27*, e1931. [CrossRef]
15. Philipp, A.; Bartholy, J.; Beck, C.; Erpicum, M.; Esteban, P.; Fettweis, X.; Huth, R.; James, P.; Jourdain, S.; Kreienkamp, F.; et al. Cost733cat–A database of weather and circulation type classifications. *Phys. Chem. Earth Parts ABC* **2010**, *35*, 360–373. [CrossRef]
16. Shu, L.; Xie, M.; Gao, D.; Wang, T.; Fang, D.; Liu, Q.; Huang, A.; Peng, L. Regional severe particle pollution and its association with synoptic weather patterns in the Yangtze River Delta region, China. *Atmos. Chem. Phys.* **2017**, *17*, 12871–12891. [CrossRef]
17. Shikhovtsev, M.Y.; Molozhnikova, Y.V.; Obolkin, V.A.; Potemkin, V.L.; Lutskin, E.S.; Khodzher, T.V. Features of Temporal Variability of the Concentrations of Gaseous Trace Pollutants in the Air of the Urban and Rural Areas in the Southern Baikal Region (East Siberia, Russia). *Appl. Sci.* **2024**, *14*, 8327. [CrossRef]
18. Molozhnikova, Y.; Shikhovtsev, M.; Khodzher, T. Results of a Comprehensive Study on Atmospheric Pollution at the Tankhoi Observation Point (Southeastern Coast of Lake Baikal, Russia): Temporal Variability and Identification of Sources. *Environments* **2025**, *12*, 462. [CrossRef]
19. Shen, M.; Tan, X. The Analysis of the Extreme Cold in North America Linked to the Western Hemisphere Circulation Pattern. *Atmosphere* **2025**, *16*, 781. [CrossRef]
20. Serrano-Notivoli, R.; Lemus-Canovas, M.; Barrao, S.; Sarricolea, P.; Meseguer-Ruiz, O.; Tejedor, E. Heat and cold waves in mainland Spain: Origins, characteristics, and trends. *Weather Clim. Extrem.* **2022**, *37*, 100471. [CrossRef]
21. Jeong, D.I.; Cannon, A.J.; Yu, B. Influences of atmospheric blocking on North American summer heatwaves in a changing climate: A comparison of two Canadian Earth system model large ensembles. *Clim. Change* **2022**, *172*, 5. [CrossRef]
22. Pérez-García, L.; García-Hernández, C.; Ruiz-Fernández, J. Trends, Atmospheric Patterns, and Spatial Variability of Heatwaves in an Oceanic Climate Area of NW Iberia. *Land* **2025**, *14*, 310. [CrossRef]
23. Lemus-Canovas, M.; Lopez-Bustins, J.A.; Martín-Vide, J.; Halifa-Marin, A.; Insua-Costa, D.; Martinez-Artigas, J.; Trapero, L.; Serrano-Notivoli, R.; Cuadrat, J.M. Characterisation of Extreme Precipitation Events in the Pyrenees: From the Local to the Synoptic Scale. *Atmosphere* **2021**, *12*, 665. [CrossRef]
24. Driouech, F. Distribution des Précipitations Hivernales sur le Maroc dans le Cadre d'un Changement Climatique: Descente D'échelle et Incertitudes (Winter Precipitation Distribution over Morocco Under Climate Change: Downscaling and Uncertainties). Ph.D. Thesis, Institut National Polytechnique de Toulouse, Toulouse, France, 2010; pp. 1–164.
25. Knippertz, P.; Christoph, M.; Speth, P. Long-term precipitation variability in Morocco and the link to the large-scale circulation in recent and future climates. *Meteorol. Atmos. Phys.* **2003**, *83*, 67–88. [CrossRef]
26. Bellichi, A. Low Frequency Winter Rainfall Variability in the North West of Morocco. In *Agricultural Adaptation to Climate Change*; Bryant, C.R., Sarr, M.A., Délusca, K., Eds.; Springer International Publishing: Cham, Switzerland, 2016; pp. 133–152. [CrossRef]
27. Lamb, P.J.; Peppler, R.A. North Atlantic oscillation: Concept and an application. *Bull. Am. Meteorol. Soc.* **1987**, *68*, 1218–1225. [CrossRef]
28. Delannoy, H. Précipitations saisonnières du Maroc cisatlasique et téléconnexions dans la circulation atmosphérique (Seasonal precipitations of the cisatlasic Morocco and teleconnections in the atmospheric circulaton). *Bull. Assoc. Géogr. Fr.* **1988**, *65*, 393–406. [CrossRef]
29. Boughdadi, S.; Ait Brahim, Y.; El Alaoui El Fels, A.; Saidi, M.E. Rainfall Variability and Teleconnections with Large-Scale Atmospheric Circulation Patterns in West-Central Morocco. *Atmosphere* **2023**, *14*, 1293. [CrossRef]
30. Knippertz, P.; Ulbrich, U.; Marques, F.; Corte-Real, J. Decadal changes in the link between El Niño and springtime North Atlantic oscillation and European-North African rainfall. *Int. J. Climatol.* **2003**, *23*, 1293–1311. [CrossRef]
31. Born, K.; Christoph, M.; Fink, A.H.; Knippertz, P.; Paeth, H.; Speth, P. Moroccan Climate in the Present and Future: Combined View from Observational Data and Regional Climate Scenarios. In *Climatic Changes and Water Resources in the Middle East and North Africa*; Zereini, F., Hötzl, H., Eds.; Springe: Berlin/Heidelberg, Germany, 2008; pp. 29–45. [CrossRef]
32. Knippertz, P.; Fink, A.H.; Reiner, A.; Speth, P. Three Late Summer/Early Autumn Cases of Tropical–Extratropical Interactions Causing Precipitation in Northwest Africa. *Mon. Weather. Rev.* **2003**, *131*, 116–135. [CrossRef]
33. Knippertz, P. A Simple Identification Scheme for Upper-Level Troughs and Its Application to Winter Precipitation Variability in Northwest Africa. *J. Clim.* **2004**, *17*, 1411–1418. [CrossRef]
34. Huebener, H.; Kerschgens, M. Downscaling of current and future rainfall climatologies for southern Morocco. Part II: Climate change signals. *Int. J. Climatol.* **2007**, *27*, 1065–1073. [CrossRef]
35. Benarafa, S. Variability and climatic impacts of weather types on Rabat. In *Aspects de la Variabilité du Climat Marocain*; Bellichi, A., Ed.; Colloques et Seminaires; Publications of the Faculty of Letters and Human Sciences-Rabat: Rabat, Morocco, 1998; pp. 49–71.
36. Noin, D. Types de temps d ' été au Maroc. *Ann. Géogr.* **1963**, *72*, 1–12. [CrossRef]

37. Delannoy, H.; Lecompte, M. Utilisation de l'analyse factorielle des correspondances pour l'etude des precipitations quotidiennes: Un exemple au Maroc. *Mediterranee* **1980**, *40*, 29–36. [CrossRef]
38. Born, K.; Fink, A.H.; Knippertz, P.P. Meteorological processes influencing the weather and climate of Morocco. In *Impacts of Global Change on the Hydrological Cycle in West and Northwest Africa*; Speth, P., Christoph, M., Diekkrüger, B., Eds.; Springer: Berlin/Heidelberg, Germany, 2010; pp. 150–163.
39. Amraoui, L. Variabilités Climatiques Régionales et Changement Global: Cas de L'évolution Climatique Récente au Maroc, en Mauritanie et sur leur Proche Océan. Ph.D. Thesis, Université Jean Moulin, Lyon, France, 2013.
40. Lemus-Canovas, M.; Lopez-Bustins, J.A.; Martin-Vide, J.; Royé, D. synoptReg: An R package for computing a synoptic climate classification and a spatial regionalization of environmental data. *Environ. Model. Softw.* **2019**, *118*, 114–119. [CrossRef]
41. Hanchane, M. Le climat du Maroc: Mécanismes, grandes zones et changements actuels. In *Nouvelle Géographie du Maroc*; Berriane, M., Ed.; Presses de l'Académie du Royaume du Maroc: Rabat, Morocco, 2025; Volume 1, pp. 51–73.
42. Hanchane, M. Maroc, Une Mosaïque de Climats. Encyclopédie de L'environnement. Available online: https://www.encyclopedie-environnement.org/air/climat-maroc/ (accessed on 14 April 2025).
43. Kanamitsu, M.; Ebisuzaki, W.; Woollen, J.; Yang, S.-K.; Hnilo, J.J.; Fiorino, M.; Potter, G.L. NCEP–DOE AMIP-II Reanalysis (R-2). *Bull. Am. Meteorol. Soc.* **2002**, *83*, 1631–1644. [CrossRef]
44. Contini, D.; Genga, A.; Cesari, D.; Siciliano, M.; Donateo, A.; Bove, M.C.; Guascito, M.R. Characterisation and source apportionment of PM10 in an urban background site in Lecce. *Atmos. Res.* **2010**, *95*, 40–54. [CrossRef]
45. Richman, M.B. Rotation of principal components. *J. Climatol.* **1986**, *6*, 293–335. [CrossRef]
46. Ekström, M.; Jönsson, P.; Bärring, L. Synoptic pressure patterns associated with major wind erosion events in southern Sweden (1973–1991). *Clim. Res.* **2002**, *23*, 51–66. [CrossRef]
47. Horel, J.D. A Rotated Principal Component Analysis of the Interannual Variability of the Northern Hemisphere 500 mb Height Field. *Mon. Weather. Rev.* **1981**, *109*, 2080–2092. [CrossRef]
48. Esteban, P.; Jones, P.D.; Martín-Vide, J.; Mases, M. Atmospheric circulation patterns related to heavy snowfall days in Andorra, Pyrenees. *Int. J. Climatol.* **2005**, *25*, 319–329. [CrossRef]
49. Esteban, P.; Martin-Vide, J.; Mases, M. Daily atmospheric circulation catalogue for western Europe using multivariate techniques. *Int. J. Climatol.* **2006**, *26*, 1501–1515. [CrossRef]
50. Ekström, M.; McTainsh, G.H.; Chappell, A. Australian dust storms: Temporal trends and relationships with synoptic pressure distributions (1960–99). *Int. J. Climatol.* **2004**, *24*, 1581–1599. [CrossRef]
51. Barbier, J.; Guichard, F.; Bouniol, D.; Couvreux, F.; Roehrig, R. Detection of Intraseasonal Large-Scale Heat Waves: Characteristics and Historical Trends during the Sahelian Spring. *J. Clim.* **2018**, *31*, 61–80. [CrossRef]
52. Francis, D.; Fonseca, R.; Nelli, N.; Cuesta, J.; Weston, M.; Evan, A.; Temimi, M. The Atmospheric Drivers of the Major Saharan Dust Storm in June 2020. *Geophys. Res. Lett.* **2020**, *47*, e2020GL090102. [CrossRef]
53. Chauvin, F.; Roehrig, R.; Lafore, J.-P. Intraseasonal Variability of the Saharan Heat Low and Its Link with Midlatitudes. *J. Clim.* **2010**, *23*, 2544–2561. [CrossRef]
54. Asutosh, A.; Vinoj, V.; Murukesh, N.; Ramisetty, R.; Mittal, N. Investigation of June 2020 giant Saharan dust storm using remote sensing observations and model reanalysis. *Sci. Rep.* **2022**, *12*, 6114. [CrossRef]
55. Hanchane, M. Different types of atmospheric circulation linked to major climatic risks in Morocco. In *Proceedings of the Conference on Risques Hydroclimatiques et Géomorphologiques: Typologie, Cartographie et Gestion*; Université Mohammed Premier (UMP), Ed.; Publications de l'Université Mohammed Premier: Oujda, Morocco, 2024; pp. 7–17.
56. Lavaysse, C.; Flamant, C.; Janicot, S.; Parker, D.J.; Lafore, J.-P.; Sultan, B.; Pelon, J. Seasonal evolution of the West African heat low: A climatological perspective. *Clim. Dyn.* **2009**, *33*, 313–330. [CrossRef]
57. Lemus-Canovas, M.; Alonso-González, E.; Bonsoms, J.; López-Moreno, J.I. Daily concentration of snowfalls in the mountains of the Iberian Peninsula. *Int. J. Climatol.* **2024**, *44*, 485–500. [CrossRef]
58. Littmann, T. An empirical classification of weather types in the Mediterranean Basin and their interrelation with rainfall. *Theor. Appl. Climatol.* **2000**, *66*, 161–171. [CrossRef]
59. Grimalt, M.; Tomàs, M.; Alomar, G.; Martin-Vide, J.; Moreno-García, M.C. Determination of the Jenkinson and Collison' s weather types for the western Mediterranean basin over the 1948–2009 period. Temporal analysis. *Atmósfera* **2013**, *26*, 75–94. [CrossRef]
60. Cresswell-Clay, N.; Ummenhofer, C.C.; Thatcher, D.L.; Wanamaker, A.D.; Denniston, R.F.; Asmerom, Y.; Polyak, V.J. Twentieth-century Azores High expansion unprecedented in the past 1200 years. *Nat. Geosci.* **2022**, *15*, 548–553. [CrossRef]
61. Ummenhofer, C.; Cresswell-Clay, N.; Thatcher, D.; Wanamaker, A.; Denniston, R.; Asmerom, Y.; Polyak, V. Unprecedented Expansion of the Azores High due to Anthropogenic Climate Change. *Eur. Geophys. Union Gen. Assem.* **2022**, EGU22-3876. [CrossRef]
62. Giuntoli, I.; Fabiano, F.; Corti, S. Seasonal predictability of Mediterranean weather regimes in the Copernicus C3S systems. *Clim. Dyn.* **2022**, *58*, 2131–2147. [CrossRef]

63. Trigo, I.F.; Bigg, G.R.; Davies, T.D. Climatology of Cyclogenesis Mechanisms in the Mediterranean. *Mon. Weather. Rev.* **2002**, *130*, 549–569. [CrossRef]
64. Alves, J.M.R.; Miranda, P.M.A.; Tomé, R.; Caldeira, R. Evolution of the subtropical surface wind in the north-east Atlantic under climate change. *Clim. Dyn.* **2024**, *63*, 3. [CrossRef]
65. Dorta, P.; Marzol, M.; Valladares, P. Localisation et fréquence des cellules de pression dans l'Atlantique Nord, l'Europe occidentale et le nord de l'Afrique (1983–1992). *Publ. L'assoc. Int. Climatol.* **1993**, *6*, 453–466.
66. Adame, J.A.; Notario, A.; Cuevas, C.A.; Saiz-Lopez, A. Saharan air outflow variability in the 1980–2020 period. *Sci. Total Environ.* **2022**, *839*, 156268. [CrossRef]
67. Davis, R.E.; Hayden, B.P.; Gay, D.A.; Phillips, W.L.; Jones, G.V. The North Atlantic Subtropical Anticyclone. *J. Clim.* **1997**, *10*, 728–744. [CrossRef]
68. Fernández-González, S.; del Río, S.; Castro, A.; Penas, A.; Fernández-Raga, M.; Calvo, A.I.; Fraile, R. Connection between NAO, weather types and precipitation in León, Spain (1948–2008). *Int. J. Climatol.* **2012**, *32*, 2181–2196. [CrossRef]
69. Chen, T.-C. Maintenance of the Midtropospheric North African Summer Circulation: Saharan High and African Easterly Jet. *J. Clim.* **2005**, *18*, 2943–2962. [CrossRef]
70. Delannoy, H. Les variations des précipitations du Maroc du Centre-ouest. *Méditerranée* **1998**, *88*, 11–17. [CrossRef]
71. Lionello, P.; Giorgi, F. Winter precipitation and cyclones in the Mediterranean region: Future climate scenarios in a regional simulation. *Adv. Geosci.* **2007**, *12*, 153–158. [CrossRef]
72. Frazão, H.C.; Prien, R.D.; Schulz-bull, D.E.; Seidov, D.; Waniek, J.J. The Forgotten Azores Current: A Long-Term Perspective. *Front. Mar. Sci.* **2022**, *9*, 842251. [CrossRef]
73. Ulbrich, U.; Christoph, M. A shift of the NAO and increasing storm track activity over Europe due to anthropogenic greenhouse gas forcing. *Clim. Dyn.* **1999**, *15*, 551–559. [CrossRef]
74. Babanov, B.A.; Semenov, V.A.; Mokhov, I.I. Comparison of Cluster Analysis Methods for Identifying Weather Regimes in the Euro-Atlantic Region for Winter and Summer Seasons. *Izv. Atmos. Ocean. Phys.* **2023**, *59*, 605–623. [CrossRef]
75. Driouech, F.; Déqué, M.; Sánchez-Gómez, E. Weather regimes-Moroccan precipitation link in a regional climate change simulation. *Glob. Planet Change* **2010**, *72*, 1–10. [CrossRef]
76. Lavaysse, C.; Flamant, C.; Evan, A.; Janicot, S.; Gaetani, M. Recent climatological trend of the Saharan heat low and its impact on the West African climate. *Clim. Dyn.* **2016**, *47*, 3479–3498. [CrossRef]
77. Carvalho, F.R.S.; Meirelles, M.G.; Henriques, D.V.; Navarro, P.V.; Vasconcelos, H.C. Climate Change and the Increase of Extreme Events in Azores. In *Handbook of Human and Planetary Health*; Leal Filho, W., Ed.; Springer International Publishing: Cham, Switzerland, 2022; pp. 349–365. [CrossRef]